Heliyon 9 (2023) e19812

Contents lists available at ScienceDirect

Heliyon

journal homepage: www.cell.com/heliyon

Integrating network pharmacology and experimental verification strategies to reveal the active ingredients and molecular mechanism of Tenghuang Jiangu Capsule against osteoporosis

Miao Li [a,c,1], Hongyu Tang [a,b,1], Yuanhao Hu [a], Songtao Li [a,c], Pan Kang [a,c], Baihao Chen [a,c], Shaocong Li [a,c], Meng Zhang [d,***], Haibin Wang [a,b,c,**], Shaochuan Huo [e,*]

[a] Guangzhou University of Chinese Medicine, Guangzhou, 510405, China
[b] Department of Joint Orthopaedic, The First Affiliated Hospital of Guangzhou University of Chinese Medicine, Guangzhou, 510405, China
[c] Lingnan Medical Research Center of Guangzhou University of Chinese Medicine, Guangzhou, 510405, China
[d] Department of Orthopedics, Henan Provincial People's Hospital, People's Hospital of Zhengzhou University, People's Hospital of Henan University, Zhengzhou, 450003, China
[e] Shenzhen Hospital (Futian) of Guangzhou University of Chinese Medicine, No.6001, North Ring Road, Futian District, Shenzhen City, Guangdong Province, 518048, China

ARTICLE INFO

Keywords:
Teng Huang Jian Gu capsule (THJGC)
Osteoporosis
Network pharmacology
Bone formation
Experimental validation

ABSTRACT

Tenghuang Jiangu Capsule (THJGC) is a Chinese herbal formula used for the treatment of osteoporosis and osteoarthritis in China, but its mechanism for treating osteoporosis is not clear. The aim of this study was to investigate the therapeutic effect of THJGC on osteoporosis and its intrinsic mechanism through network pharmacology and experimental validation. Drugs and potential targets were obtained from several reliable databases through network pharmacology, and these targets were integrated and analyzed using bioinformatics and molecular docking strategies. Quercetin, lignans and kaempferol were identified as key components, and the key targets included Akt1, MAPKs, and CASP3. Subsequently, UPLC-MS/MS analysis confirmed the presence of components in THJGC for the treatment of osteoporosis. In addition, using ex vivo and in vivo models, it was confirmed that THJGC inhibited H_2O_2-induced ROS generation and apoptosis, and reduced OVX-induced bone loss in a mouse model of osteoporosis. Our data suggest that THJGC has antioxidant, bone formation-promoting, bone resorption-inhibiting, and MC3T3-E1 apoptosis-reducing effects, and thus has anti-osteoporotic properties. In conclusion, it may be a promising pharmacologic adjuvant treatment for osteoporosis.

* Corresponding author.
** Corresponding author. Department of Joint Orthopaedic, The First Affiliated Hospital of Guangzhou University of Chinese Medicine, Guangzhou, 510405, China.
*** Corresponding author.
E-mail addresses: zhangmeng.lh@163.com (M. Zhang), hipman@163.com (H. Wang), huoshaochuansz@163.com (S. Huo).
[1] These authors contributed equally to this work.

https://doi.org/10.1016/j.heliyon.2023.e19812
Received 24 March 2023; Received in revised form 1 September 2023; Accepted 1 September 2023
Available online 4 September 2023
2405-8440/© 2023 The Authors. Published by Elsevier Ltd. This is an open access article under the CC BY-NC-ND license (http://creativecommons.org/licenses/by-nc-nd/4.0/).

1. Introduction

Osteoporosis (OP) is a systemic metabolism bone disorder characterized by low bone mass and degeneration of bone microstructure, resulting in reduced bone strength and increased fracture risk [1,2]. Globally, more than 200 million individuals suffer from osteoporosis, making it a serious public health concern [3]. The prevalence of osteoporosis has increased dramatically with the aging of the population, posing significant health risksand financial burdenon the elderly and society. In spite of the advancement of newer drugs in treating osteoporosis, there are still no effective therapeutic approaches available to reverse the pathogenesis of osteoporosis. Moreover, the side effects associated with long-term use remain a substantial challenge [4]. Therefore, it is of great importance to discover and develop drugs with fewer side effects to improve clinical outcomes in osteoporosis treatment.In recent years, Traditional Chinese medicine (TCM) has been widely used to prevent and treat a variety of diseases due to its satisfactory clinical efficacy and fewer adverse reactions [5]. Accumulating evidence suggests that TCM can reduce bone loss, increase bone density, and decrease the incidence of fragility fractures, showing apparent beneficial effects on osteoporosis [6,7].

TenghuangJiangu Capsule (THJGC) is a proprietary Chinese medicine for the treatment of bone and joint diseases approved by The State Food and Drug Administration (SFDA) of China (Approval number: Z20123001). It consists of YYH (*Epimedium brevicornu* Maxim), GSB (*Drynaria fortunei*(Kunze)J.Sm), RCR(*Cistanche deserticola* Y.C. Ma), LXC(*Pyrola calliantha* H.AndreS), SDH(*Rehmannia glutinosa* Libosch),JXT(*Spatholobus suberectus* Dunn), and LFZ(*Raphanus sativus*.L) (Table 1). In China, THJGC combined with zoledronic acid or Chinese acupuncture has been reported to be used in the treatment of primary osteoporosis [8,9]. A review by Indran et al. concludes that compounds of Yinyanghuo has significant efficacy in the treatment and prevention of osteoporosis and bone health [10]. Kang et al. confirmed the anti-osteoporosis effect of Gusuibu extract [11]. What's more, Liang et al. reported that Cistanches Herba aqueous extract can regulate the serum bone metabolites of patients with osteoporosis [12]. According to the review written by Liu et al., those formulas contain Dihuang will enhance the effect of anti-osteoporosis [13]. Previous studies also have shown that the active components of THJGC, such as icariin, kahanol, luteolin and quercetin, can promote osteogenic differentiation and bone formation, and inhibit osteoclast differentiation and bone resorption [14–16]. However, potential effects of THJGC on osteoporosis and its underlying mechanisms remain unclear.

Due to the complexity of Chinese medicine prescription, there is still a long way to reveal the therapeutic compositions and deep mechanisms of TCM. Network pharmacology has recently emerged as an important tool for analyzing the mechanism of traditional Chinese herbs thanks to the generalization of systems biology. In the present study, we explored the effect of THJGC on ovariectomized mice by using network pharmacology, molecular docking strategy, and Micro-CT reconstruction technology. The information obtained in this study will help clarify the effect and mechanisms of THJGC in the treatment of osteoporosis and its underlying therapeutic compositions. Maybe we can develop it as a new possible drug adjuvant therapy for osteoporosis in the future.

2. Materials and methods

2.1. Screening of active ingredients and targets

The active ingredients of THJGC and their corresponding targets were screened by searching the Traditional Chinese Medicine Systems Pharmacology Database (TCMSP, https://tcmsp-e.com/) [17]. Only ingredients fulfilling the screening criteria of both oral bioavailability $\geq$30% and drug-likeness $\geq$0.18 were selected for further analysis. The Uniprot database (https://www.uniprot.org/) was applied to convert target names to their corresponding official gene symbols.

2.2. Collection of osteoporosis related targets

We searched the OMIM database (https://www.omim.org/) and GeneCards database (https://www.genecards.org/) to obtain targets associated with osteoporosis [18,19]. After removing the duplicate targets from the two databases, we finally acquired all targets related to osteoporosis. The intersection targets of THJGC and osteoporosis, which were identified as candidate targets, were displayed with a Venn diagram.

2.3. Construction of networks

The candidate targets were imported into STRING database (https://string-db.org/) to construct PPI(Protein Protein interaction)

Table 1
The ingredients of the Tenghuang jiangu capsule.

Chinese name	Botanical names	The proportion of ingredients (100%)
YYH	*Epimedium brevicornu* Maxim	14.3
GSB	*Drynaria fortune* (Kunze)J.Sm	14.3
RCR	*Cistanche deserticola* Y.C. Ma	14.3
LXC	*Pyrola calliantha* H.AndreS	14.3
SDH	*Rehmannia glutinosa* Libosch	21.4
JXT	*Spatholobus suberectus* Dunn	14.3
LFZ	*Raphanus sativus*.L	7.1

network with a combined confidence score higher than 0.4 [20]. The PPI network was further analyzed and visualized by applying Cytoscape software [21]. Subsequently, the network of ingredients and corresponding targets of each herb in THJGC were generated for visual analysis. In the network, the nodes with diverse colors and shapes represented different herbs, targets, and active ingredients.

2.4. Gene functional enrichment analysis of THJGC for osteoporosis

The Gene Ontology (GO) function and Kyoto Encyclopedia of Genes and Genomes (KEGG) pathway analysis were carried out based on the candidate targets. The functional enrichment analysis for GO terms includes molecular functions (MF), biological processes (BP), and cellular components (CC). The top 20 terms with the highest enrichment of each category were presented in the visual graphics by R software.

2.5. Molecular docking

On the basis of the results of bioinformatics analysis, key targets and candidate ingredients were selected to perform molecular docking. The mol2 format structures of the candidate ingredients were obtained from TCMSP database, and the crystal structures of the key targets were obtained from RCSB database (http://www.rcsb.org/). After removing water, adding polar hydrogen atoms, and extracting the ligand structureby using Pymol software, docking validation was completed by Autodock software (Version1.1.2) [22]. The binding activity between the targets and the active ingredients was evaluated and visualized using Discovery Studio 2020 [23].

2.6. UPLC-MS/MS analysis

Ultra-performance liquid chromatography-tandem mass spectrometry method was used for the detection and analysis of THJGC sample solution. The main parameters are as follows: chromatographic column was Waters ACQUITY UPLC BEH C18(2.1 × 50 mm); column temperature was set at 35 °C.The column flow rate was 0.3 ml/min. The mobile phases of HPLC were composed of water (A) and acetonitrile (B). PDA detection was set as 200–360 nm continuous scanning. 5 g of sample was accurately weighed and placed in a 10 ml centrifuge tube, 4.0 ml of 70% ethanol solution was added, they were soaked for 2 h at room temperature and then ultrasonic extraction was carried out for 30 min. The upper extract was collected after centrifugation at 10000 rpm and then 4.0 ml of 70% ethanol solution was added for ultrasonic extraction. 70% ethanol water solution was used to dilute and the test solution obtained by 0.2 μm microporous membrane filter.

2.7. Cell culture and drug intervention

MC3T3-E1 cells were purchased from Procell (Wuhan, China) and maintained in α-MEM medium supplemented with 10% fetal bovine serum,100 U/mL penicillin and 100 U/mL streptomycin at 37 °C in a humidified atmosphere of 5% CO_2. After reaching confluence, the cells were pretreated with different concentrations of THJGC with or without 200 μM/L H_2O_2 for 2 h. THJGC was dissolved in dimethylsulfoxide (DMSO) and diluted to different concentrations for in vitro experiments.

2.8. Cell viability detection

The cell viability was detected using the Cell Counting Kit-8 (Biosharp, China) according to the manufacturer's protocol.Briefly, MC3T3-E1 were cultured for 24 h in 96-well plates and then treated with different concentrations of THJGC(0.25, 0.5, and 1 μg/mL). After intervention for 24 h, 10 μl of CCK-8 solution was added into each well and incubated for another 2 h. The absorbance of the wells was measured and recorded at 450 nm with microplate reader.

2.9. Caspase3 enzyme activity assay

Proteins were extracted from cells after drug intervention by adding Ripa lysate without protease inhibitors, and samples of the same concentration were prepared after determination of protein concentration using a BCA kit (P0010S, Beyotime). The pNA standard curve was determined according to the Caspase3 enzyme activity assay kit (C1157, Beyotime), and after preparing the sample system according to the kit, the OD value at 405 nm was measured using an enzyme marker. Finally, the pNA content in the samples was calculated according to the standard curve.

2.10. Apoptosis detection assay

The Annexin V-FITC/PI kit was used to assess apoptosis. After the intervention, cells were digested, washed twice with PBS and then incubated with Annexin V-FITC and PI for 5 min at room temperature in a light-protected environment, followed by detection using a FACSCanto II flow cytometer (BD Biosciences, USA).

2.11. Determination of ROS in MC3T3-E1

After drug intervention for 24h, MC3T3-E1 cells were incubated with 200 μM/L H_2O_2 for 2 h in the presence or absence of THJGC

(0.25, 0.5 μg/mL). Cells were then washed with PBS and incubated with 10 μM DCFH-DA for 30 min at 37 °C. ROS-positive cells were captured with fluorescence microscope.

2.12. Quantitative reverse transcription (qRT)-PCR analysis

Total RNA from cultured cells was extracted using Trizol reagent, and 1 μg of RNA was reverse transcribed into cDNA using a reverse transcription kit (RR036A, Takara) according to the manufacturer's protocol. Quantitative analysis was carried out using (AG11701, AG) with the CFX96 real-time PCR detection system (Bio-Rad). The relative mRNA expression of genes was normalized to the level of internal control GAPDH. All primers were listed in Table 2.

2.13. Animal experimentation

Eighteen 49-day-old female C57/BL6 mice (20 ± 2 g) were provided by the Animal Experiment Center of Guangzhou University of Traditional Chinese Medicine (SCXK(GD)2018-0034). After 7 days of acclimatization feeding, they were divided into 3 groups according to the principle of random assignment: Sham-operation group (sham-operation in week 8 + postoperative daily instillation of an equal amount of saline), OVX group (OVX-operation in week 8 + postoperative daily instillation of an equal amount of saline), and THJGC group (OVX-operation in week 8 + postoperative daily instillation of 360 mg/kg of THJGC).The dosage used for THJGC was determined by the accepted body surface area conversion method was obtained [24]. All animals used in this study were kept in the SPF Laboratory Animal Center (SYXK (Yue) 2018-0092) of the First Affiliated Hospital of Guangzhou University of Traditional Chinese Medicine. Here there was sufficient food and normal day and night cycles. All mice were gavaged from week 9. Animals were euthanized by an overdose of anesthetic (pentobarbital) at 16 weeks of age and leg bones were removed for subsequent in vivo experiments.

2.14. Western blot

We randomly selected three right leg bones in each subgroup. Grinding was performed at −80 °C. Bone samples were lysed in RIPA buffer (P0012C Beyotime) with 1% PMSF and 1% phosphatase inhibitor (P1050, Beyotime). The BCA kit (P0010S, Beyotime) was then employed to assess the protein concentrations. Each sample containing 20 μg of total protein was separated by SDS-PAGE, and then transferred to PVDF membranes (IPVH00010, Millipore). After blocking with 5% BSA for 1 h, the membranes were incubated at 4 °C overnight with primary antibodies.Subsequently, the membranes were washed and incubated with corresponding secondary antibodies at room temperature for 1 h. Protein bands were incubated with enhanced chemilumin escence reagent and visualized using a Bio-Rad imaging system. Each set of samples was repeated once for a total of three sets of samples (n = 3). Primary antibodies included *AKT1*(bs-52010R, Bioss), *p-AKT1*(bs-0876R, Bioss), *β-Actin* (WL01372, Wanleibio), *ERK1/2*((WL01864, Wanleibio), *p-ERK1/2* (WLP1512, Wanleibio), *JNK1*(WL05246, Wanleibio), *p-JNK1*(01813, Wanleibio), *Runx2*(WL03358, Wanleibio), *NFATc1*(WL01632, Wanleibio), *Caspase3*(WL04004, Wanleibio).

2.15. Ovariectomy (OVX)-induced osteoporosis mouse model

All in vivo experiments were conducted in accordance with protocol approved by the Ethics Committee of the First Affiliated Hospital of Guangzhou University of Chinese Medicine (approval number: 2019009). Eight-week-old female C57/BL6J mice were randomly assigned into three groups (n = 6 per group): sham group, OVX group and THJGC group. After one week of adaptive feeding, bilateral oophorectomy was performed to induce osteoporosis on the mice in OVX and THJGC groups according to a previously reported method [25]. Drug intervention was started one week after surgery, the dosage of drug was counted according to the conversion method of body surface area described in the former study [24]. After surgery, mice in THJGC group were intervened with 0.4 g/kg THJGC once a day for 6 weeks, mice in sham and OVX groups were intervened with the equivalent volume of normal saline.

2.16. Micro-CT analysis

The collected femurs from the mice were fixed in 4% paraformaldehyde (PFA) for 48 h and scanned using a Skyscan 1176 micro-CT scanner (Bruker micro-CT, Kontich, Belgium) at 50 kV/500 μA following the guidelines. The raw images were reconstructed to obtain the two and three-dimensional bone structure images.The region of interest (ROI) in distal femurs was selected to measure the following trabecular bone parameters including mean volumetric bone mineral density (BMD), structure model index (SMI),bone

Table 2
Quantitative real-time PCR primer sequences.

Genes	Forward (5′-3′)	Reverse (5′-3′)
Bcl2	TGAGTACCTGAACCGGCATC	CCCAGGTATGCACCCAGAGT
Bax	GATCCAAGACCAGGGTGGCT	TCCCCCATTCATCCCAGGAA
Caspase3	GCTTGGAACGGTACGCTAAG	TCCGTACCAGAGCGAGATGA
GAPDH	CTCAGGAGAGTGTTTCCTCGT	TGATGTTAGTGGGGTCTCGC

volume/tissue volume (BV/TV), trabecular thickness (Tb. Th), trabecular spacing (Tb.Sp), and trabecular number (Tb.N).

2.17. Hematoxylin-eosin staining assay

The above fixed samples were decalcified in 14% ethylenediaminetetraacetic acid for 1 week. After decalcification, sections were embedded in paraffin and cut into 5 μm thick sections. Sections were stained with H&E and scanned with a panoramic Midi digital slide scanner (3DHISTECH Ltd., Hungary).

2.18. Statistical analysis

All statistical data were analyzed by GraphPad Prism (version 7.0) and presented as mean ± SD. Statistically differences between groups were analyzed by one-way analyses of variance (ANOVA). $P < 0.05$ was considered statistically significant.

3. Results

3.1. Candidate targets and PPI network analysis

A total of 85 active ingredients of THJGC were obtained from the TCMSP databasebased on the screening criteria, including 18 from DrynariaeRhizoma, 24 from SpatholobusSuberectus Dunn, 3 from Raphani Semen, 9 from HerbaPyrolae, 6 from CistanchesHerba, 2 from Rehmanniae Radix Praeparata, and 23 from EpimrdiiHerba.Subsequently, 241 corresponding targets of active ingredients were predicated after removing duplication(Supplementary Table S1). In addition, 5458 targets related to osteoporosis were identified through screening the disease-related database. Eventually, a total of 183 intersection targets were obtained for subsequent analysis as displayed by a Venn diagram (Fig. 1A). Following this, a PPI network of the target candidates was constructed and visualized, which consisted of 243 nodes and 1465 edges (Fig. 1B). On the basis of degree value, the top 10 significant targets in the PPI network were Akt1, MAPK3, IL6, VEGFA, CASP3, JUN, EGFR, MAPK8, EGF, and MAPK1, which were considered to be the key targets of THJGC for the treatment of osteoporosis.

3.2. Construction and analysis of the ingredient-target network

By using Cytoscape, an ingredient-target network consisting of 248 nodes and 1294 edges was constructed to explore the relationship between active ingredient and related targets. As shown in Fig. 2, the blue diamond represents potential target of drugs against osteoporosis, the circles stand for 7 drugs and their active ingredients. The nodes with more connecting ingredients or targets were shown with larger sizes, indicating their crucial role in the whole network. In the network, important ingredients such as quercetin, luteolin, and kaempferol exhibited the highest correlation with osteoporosis targets based on the degree value.

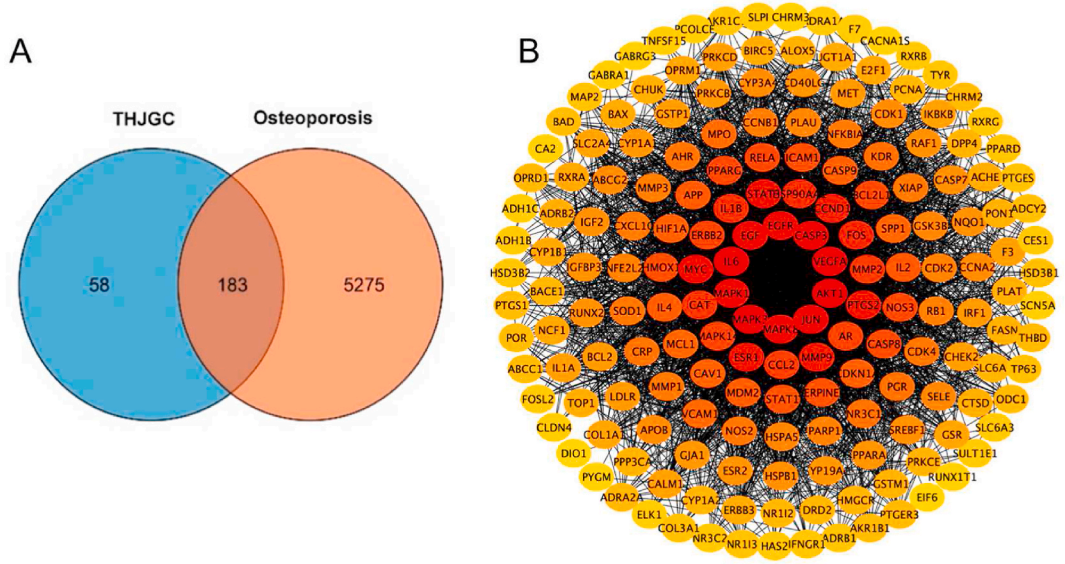

Fig. 1. Acquisition and network analysis of candidate targets of THJGC in treating osteoporosis. **(A)** A Venn diagram was performed to obtain the candidate targets of THJGC and osteoporosis. **(B)** PPI network of 183 candidate targets. Higher degrees indicated larger node sizes, red indicates higher degree and orange represents the lower degree.

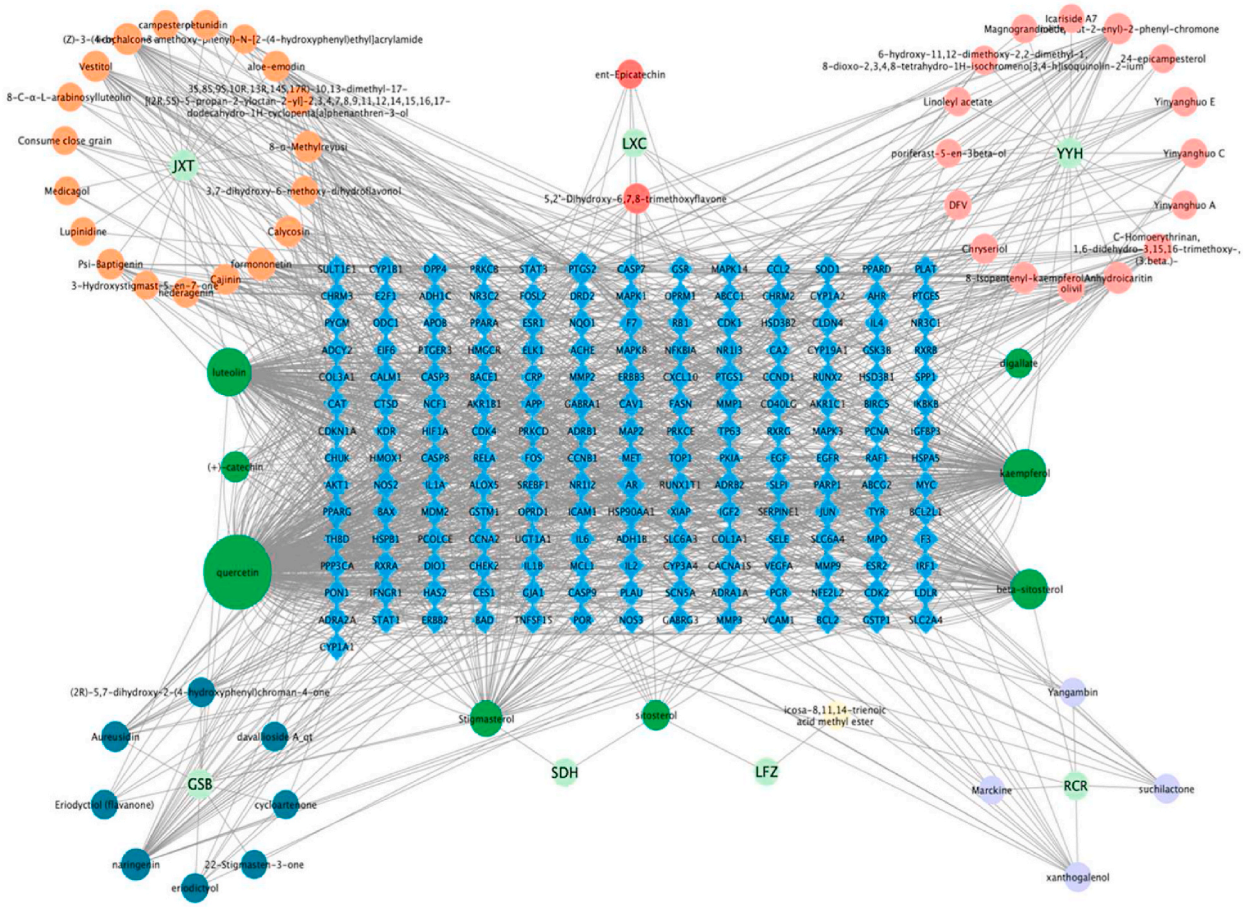

Fig. 2. Ingredient-targetnetwork analysis. Different sizes and lines density represent possibilities of all candidate targets.

3.3. GO enrichment analysis

Results of functional enrichment indicated that the candidate targets were markedly enriched in 2079 GO terms. BP enrichment mainly included response to oxidative stress, response to metal ion, response to nutrient levels, etc. CC enrichment mainly included focal adhesion, cell-substrate adherens junction, cell-substrate junction, etc. MF enrichment mainly included ubiquitin protein ligase binding, small conjugating protein ligase binding, cell adhesion molecule binding, etc.The top 20 significantly enricheditems of GO enrichment were visualized by a bubble chart (Fig. 3).

3.4. KEGG and gene-pathway network analysis

As revealed by KEGG pathway enrichment analysis, the candidate targets mainly involved in the PI3K/Akt signaling pathway, TNF signaling pathway, and Apoptosis signaling pathway. Notably,the PI3K/Akt signaling pathway contained the most key targets, indicating its importance in the treatment of osteoporosis by THJGC. The top 20 significantly enriched items of KEGG enrichment were visualized by a bubble chart (Fig. 4A). The gene-pathway network was then constructed by using Cytoscape, which contained 123 nodes and 530 edges (Fig. 4B). In the network, the orange circle nodes denote genes, and V-shapes represent pathways. The size of shape represents the degree of association between genes and pathways. The network showed that Akt1, NF-κB and MAPKs had bigger BC, and were considered as core target genes. Further, several other genes also displayed higher BC, including STAT1, STAT3, JUN, MDM2, RELA, MMP9, CCND1, RAF1, FOS, BAD, BAX, and CASP3, suggesting that they are also potential key targets for THJGC against osteoporosis.

3.5. Molecular docking verification

Molecular docking was applied to validate the binding action mode of the key targets with quercetin, luteolin, and kaempferol. Based on the degree of match of the key targets, we show the higher ranked ones in Fig. 5 A, for example, the structure of quercetin can

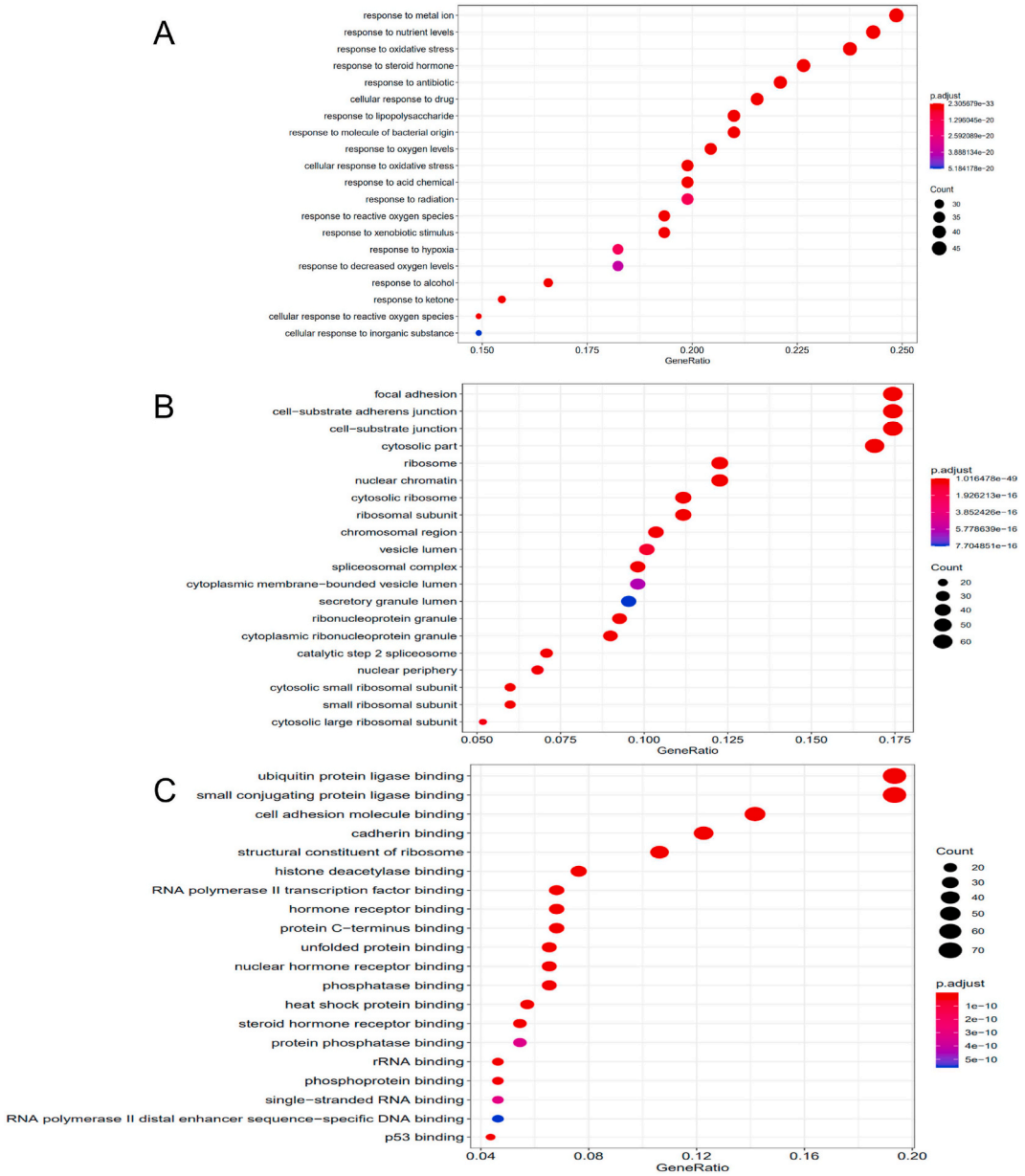

Fig. 3. GO enrichment analysis of the candidate targets. **(A)** The top 20 terms of biological process (BP) were displayed with a bubble chart. **(B)** The top 20 terms of cellular component (CC) were displayed with a bubble chart. **(C)** The top 20 terms of molecular function (MF) were displayed with a bubble chart.

form two hydrogen bonds, two π-anion bonds and one π-sigma bond with Asp292, Glu191, Glu198, Leu295 and Gly311 in AKT1. The binding energy was counted to assess the matching degree of the selected ingredients to the key targets. The detail binding energy score was displayed with a heatmap (Fig. 5B). The results indicated that the top three ingredients could bind to the active site of protein targets.

3.6. UPLC-MS/MS analysis validation of anti-osteoporosis focused components

We subjected THJGC to UPLC-MS/MS analysis and detected 61 compounds (see Table S1 for specific data), and then based on the ingredient-target network analysis conducted by our previous network pharmacology (Fig. 2), we performed qualitative analysis of the top three anti-osteoporosis ranked ingredients: quercetin, luteolin, and kaempferol were analyzed qualitatively (Fig. 6A and B) with quantitative analysis (Table 3).

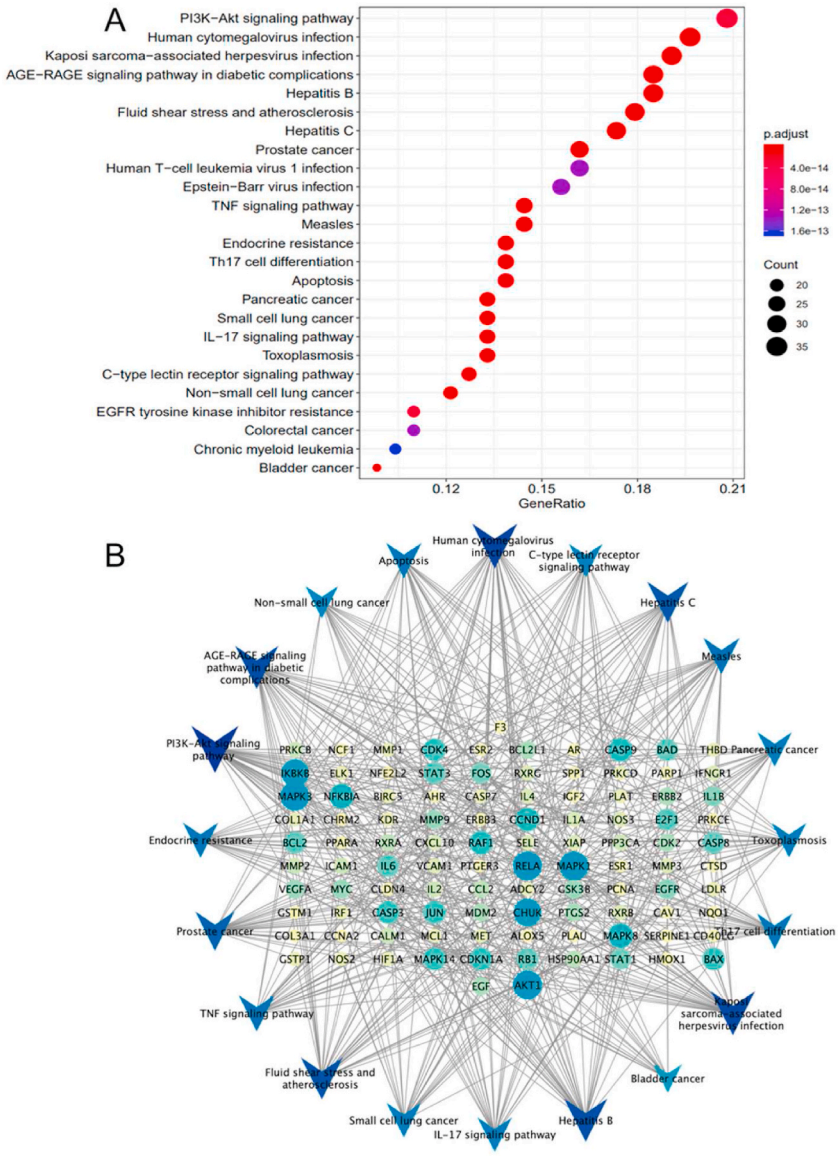

Fig. 4. KEGG pathway enrichment and gene-pathway network of the candidate targets of THJGC in treating osteoporosis. **(A)**The top 20 enriched KEGG pathways were presented with abubble chart.Size of the spot represents number of genes and color represents *P* value.**(B)** Gene-pathway network including 25 pathways and 103 genes were constructedbased on degree value. The orange circles represent target genes and the V-shapes represent pathways. Big size represents the larger degree.

3.7. THJGC exhibits no cytotoxicity on MC3T3-E1 cells

The cytotoxic effects of THJGC on MC3T3-E1 were determined at the increasing concentrations (0, 0.25, 0.5, 1 μg/ml) for 24 h. As shown in Fig. 7, THJGC was not cytotoxic to MC3T3-E1 at concentrations up to 1 μg/ml. Therefore, 0.25 and 0.5 μg/ml THJGC were used for subsequent experiments.

3.8. THJGC inhibits H_2O_2-induced apoptosis and reactive oxygen species (ROS) production

To further validate the mechanism predicted by GO analysis (BP enrichment), the relationship between the level of ROS and apoptosis-related gene expression was investigated. As shown, H_2O_2 stimulation significantly increased ROS production (Fig. 8D and E), promoted the expression of Bax and Caspase-3, and downregulated Bcl-2 expression in MC3T3-E1 cells (Fig. 8F). However, THJGC was found to reduce the number of ROS-positive cells and alter the activity of apoptosis-related genes. The results of apoptotic flow phenotypes also showed that although the rate of late apoptosis was not significant under oxidative stress conditions, the results of

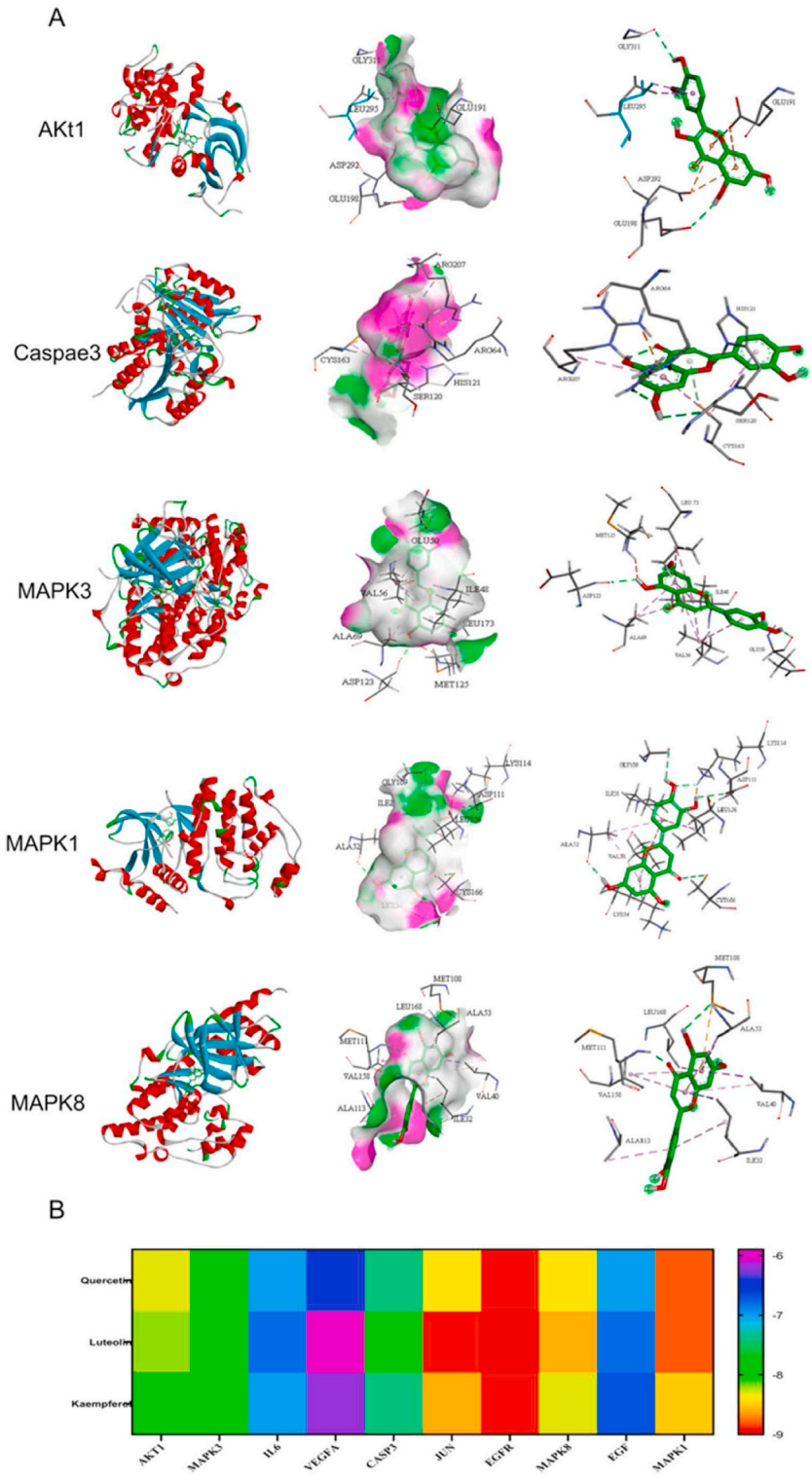

Fig. 5. Molecular docking verification of the selected ingredients to the key targets. **(A)** Mode of action of Akt1, Caspase3, MAPK1, MAPK3, MAPK8 interacting with quercetin, luteolin, and kaempferol. **(B)**The detail binding energy score was displayed with a heatmap.

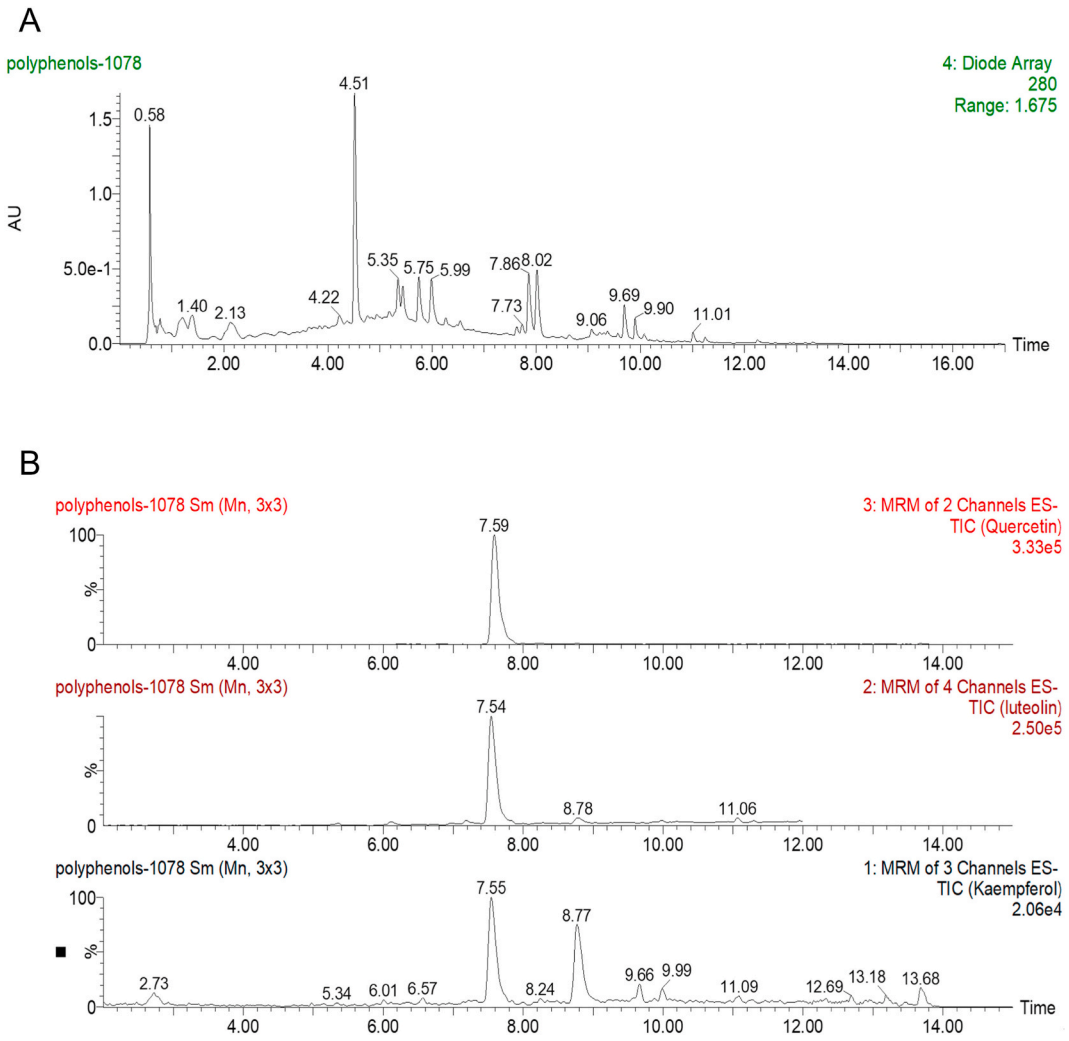

Fig. 6. UPLC-MS/MS analysis Validation of anti-osteoporosis focused components. (A) Mass spectrometric MRM detection of total ion flow chromatograms. (B) Characteristic ion chromatograms of three important anti-osteoporotic components: quercetin, luteolin, and kaempferol.

Table 3
Quantitative analysis of luteolin, Quercetin, Kaempferol.

Name	Quan Trace	RT	Conc.	Sample contents(ug/g)
luteolin	285.107 > 133.09	7.59	0.306	3.3842
Quercetin	300.825 > 178.944	7.64	1.053	11.6457
Kaempferol	285.1 > 229.15	8.81	0.15	1.6589

drug reversal were still appreciable (Fig. 8D and E). We then further examined the intracellular caspase-3 enzyme activity, and the results unsurprisingly remained consistent with the previous results (Fig. 8C).

3.9. THJGC regulates OVX-induced osteogenic differentiation and apoptosis in mice

In vitro experiments showed that THJGC has significant anti-apoptotic and antioxidant abilities. To further explore their in vivo effects, we used mouse bone tissue proteins for in vivo validation. As shown in Fig. 9A and B, the results were as we imagined, THJGC decreased the expression of osteoclast marker protein NFATc1 and increased the expression of osteoblast marker protein RUNX2, thus exerting its role in regulating osteogenesis. More interestingly, in agreement with our enrichment analysis, THJGC promoted zero acidification levels of Akt1 as well as ERK1/2 and very significantly reduced phosphorylation levels of JNK1, as well as caspase3 upon activation. It revealed a positive effect of THJGC in reducing apoptosis rate and antioxidant. Therefore, we conclude that THJGC

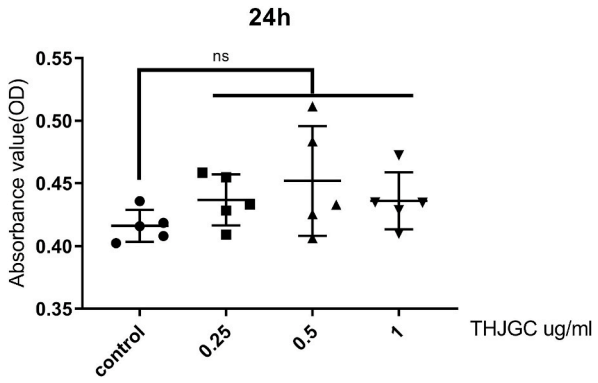

Fig. 7. Effect of THJGC on the cell viability of MC3T3-E1 cells. Cells were cultured with different concentrations of THJGC for 24 h, and cell viability was detected by CCK-8 assay.

regulates OVX-induced osteogenic differentiation and apoptosis in mice.

3.10. THJGC prevents OVX-induced bone loss in vivo

As demonstrated by micro-CT analysis, OVX was found to be responsible for an impairment in trabecular bone micro-architecture. However, treatment with THJGC significantly increased the number of bone trabeculae and improved trabecular connectivity (Fig. 10A). Quantitative analysis demonstrated that skeletal parameters including BMD, BV/TV, Tb.Th, and Tb.N in the OVX group were significantly decreased, while Tb.Sp were increased compared with the sham group. In contrast, the THJGC group exhibited an increase in BMD, BV/TV, and Tb.N, as well as a decrease in Tb.Sp compared with the OVX group. Nonetheless, no apparent differences were observed between the three groups in terms of SMI (Fig. 10B). The HE staining results showed that mice that had completed the detrusor procedure contained a large number of lipid droplets, with discontinuous bone trabeculae and greatly reduced numbers, and that after THJGC treatment, the adipocytes were significantly reduced, the bone marrow cavity was restored, and the bone trabeculae were more orderly (Fig. 10C).

4. Discussion

With the aging of the population, osteoporosis is becoming a serious public health concern. It is evident that osteoporosis fractures, which place a heavy burden on health care, are on the rise [26]. Although new and effective therapies are available for the prevention and treatment of osteoporosis, there is still need to find new treatment strategies to prevent and treat osteoporosis. The pathology of osteoporosis involves multiple targets and pathways, which may account for the limited efficacy of single-target drugs than expected. In recent years, THJGC has been found to have clinical capabilities for the treatment of osteoporosis and degenerative bone diseases [8]. However, the intrinsic mechanism of THJGC for the treatment of osteoporosis has not been reported. In the present study, the predictive results of network pharmacology and validation experiments were applied to investigate the intrinsic mechanism of THJGC against osteoporosis.

Based on the results of network pharmacology experiments, quercetin, luteolin, and kaempferol were identified as representative components that may play key role in the treatment of osteoporosis with THJGC. Quercetin is a flavonoid with a variety of biological activities, including antitumor, anti-inflammatory, antioxidant, and anti-apoptotic. Related studies have revealed the contribution of quercetin in promoting osteogenic differentiation and reducing bone loss by regulating MAPKs and PI3K/AKT signaling pathways [27,28]. Previous study had shown that luteolin significantly inhibited oxidative stress-induced apoptosis of osteoblasts and promoted osteogenetic differentiation by regulating the ERK/Lrp-5/GSK-3β signaling pathway [29]. Kaempferol is reported to effectively inhibit bone resorption and promote bone formation, implying a great potential in the maintenance of bone metabolic homeostasis [30,31]. In our current study, using functional enrichment analysis and molecular docking, we found that the candidate targets are mainly involved in biological processes such as chemical stress and steroid hormones. KEGG analysis revealed that the PI3K/Akt pathway, MAPKs (Mainly ERK1/2, JNK1 pathways) signaling pathway, and apoptosis signaling pathway were significantly enriched, which are closely related to the onset and progression of osteoporosis [32,33]. Meanwhile, THJGC was also able to reduce H_2O_2-induced oxidative damage in osteogenic precursor cells and decreased the level of ROS. Furthermore, although our current main research focus is on oxidative stress and apoptosis, which can be considered a limitation of our current study, in vivo blotting experiments have likewise demonstrated the inhibitory effect of THJGC on bone resorption. These results suggest that THJGC encompasses but is not limited to the actions of the major drug components listed above. It may exert its anti-osteoporosis effects through multiple components, multiple targets and multiple biological processes. Their pharmacological effects cannot be regarded as independent actions, but form an interacting pharmacological network, which is the advantage of traditional Chinese medicine (TCM) in the treatment of diseases such as osteoporosis [34].

ROS, which are generated accidently as by-products of aerobic metabolism, play a vital role in the regulation of cell proliferation,

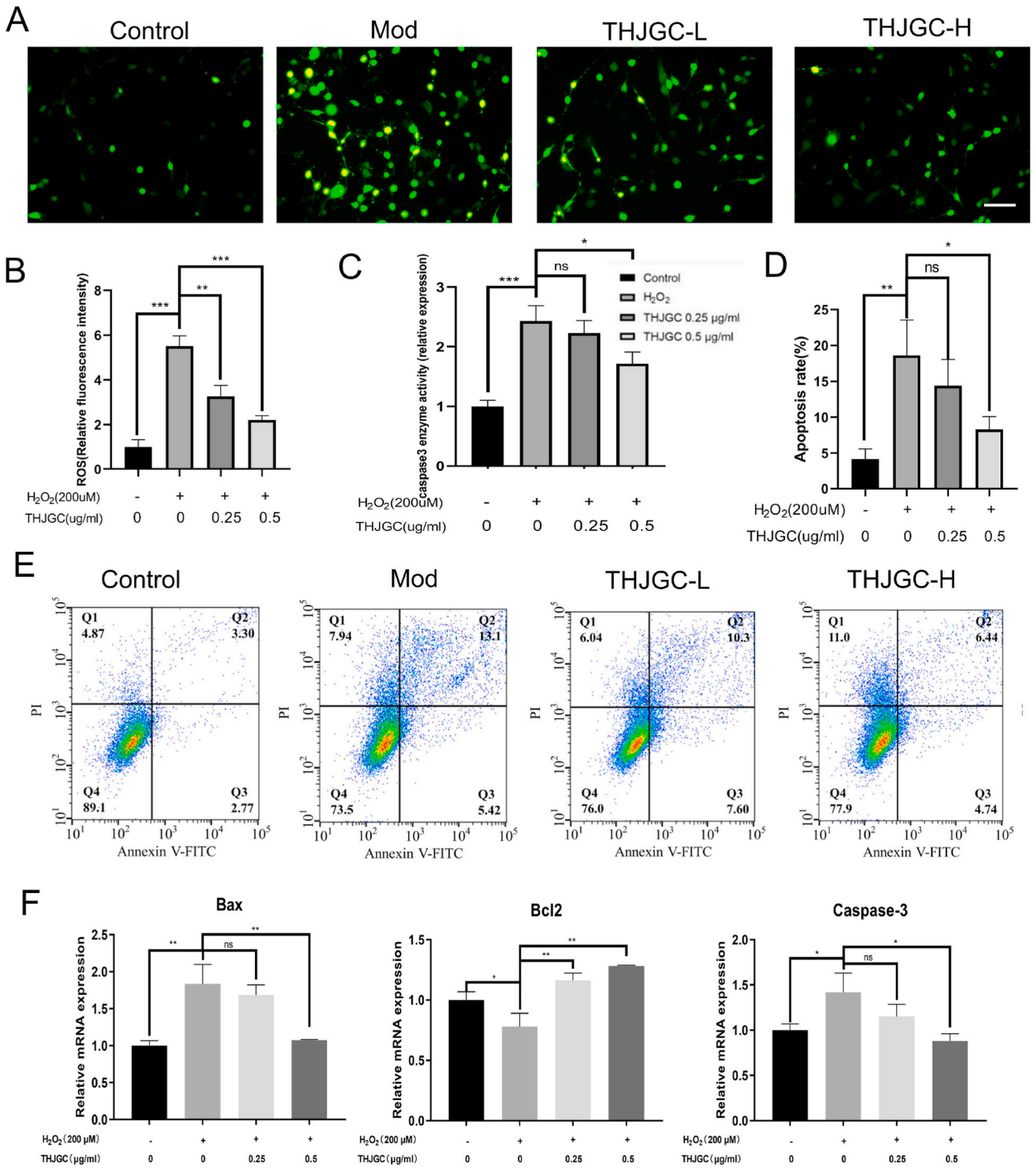

Fig. 8. THJGC inhibits H_2O_2-induced apoptosis and reactive oxygen species (ROS) production. (A) ROS production was detected with a DCFH-DA probe, and the relative fluorescence intensity of ROS was quantified in Figure (B). Scale bar = 100 μm. (C) Quantitative statistical plot of caspase3 enzyme activity assay. (E) Treatment with H_2O_2 with or without THJGC intervention for 24hr, Annexin V-FITC/PI apoptosis staining and assayed by flow cytometry. Percentage of apoptosis is shown in Figure (E). (F) Expression of apoptosis-related genes, including Bax, Bcl-2, Caspase3. The sample size of all the above experiments was three (n = 3), and each experiment was repeated 3 times. All data was demonstrated as mean ± SD, *P < 0.05, **P < 0.01, ***P < 0.001.

migration, differentiation, and apoptosis. Recently, increasing evidence indicates that ROS are involved in the metabolic regulation of osteoblasts and osteoclasts [35,36]. Overproduction of ROS contribute to the pathogenesis of osteoporosis, resulting inoxidative damage to osteoblasts and sustained bone degeneration [37]. ROS can affect the PI3K/Akt signaling pathway by influencing the

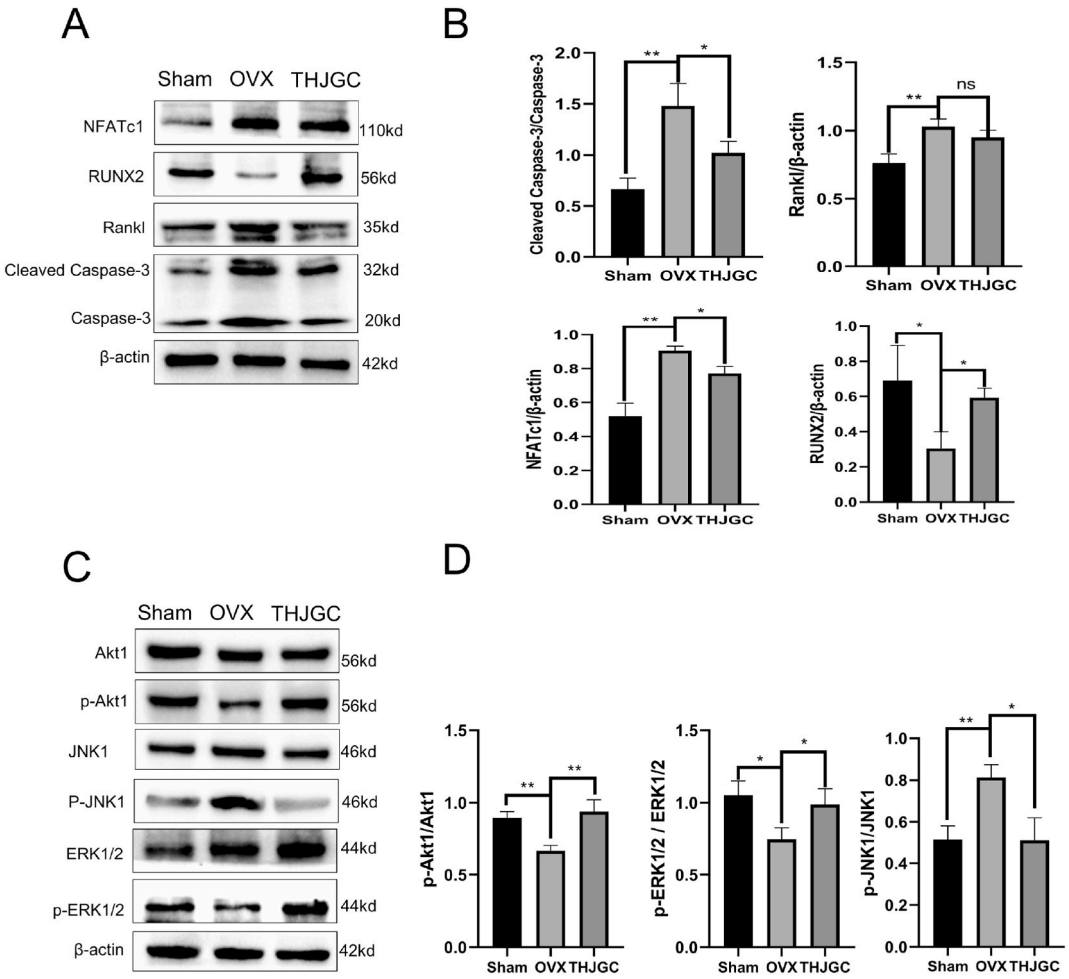

Fig. 9. THJGC regulates OVX-induced osteogenic differentiation and apoptosis in mice. (A) The protein expression levels of NFATc1, RUNX2, Rankl, and cleaved Caspase/Caspase3 in the bone tissues of mice from three groups (sham-operated group, n = 3; model group, n = 3; and THJGC group, n = 3) were analyzed by Western blotting, and the quantitative statistical analyses are shown in Figure (B). (C) The protein expression levels of *p*-Akt1/Akt1, *p*-ERK1/2/ERK1/2, and *p*-JNK1/JNK1 in the bone tissues of mice from three groups (sham-operated group, n = 3; model group, n = 3; and THJGC group, n = 3) were analyzed by Western blotting, and the quantitative statistical analyses are shown in Figure (D). All data was demonstrated as mean ± SD, *P < 0.05, **P < 0.01.

phosphorylation levels of PI3K and Akt and the expression of downstream apoptosis-related genes, and previous studies have shown that the ERK1/2 pathway is also associated with oxidative stress [38,39]. To confirm these two pathway changes in MC3T3-E1 cells, we intervened with H_2O_2 to create a model of oxidative damage and, as expected, ROS measurements provided evidence that THJGC treatment effectively reduced H_2O_2-induced ROS production and inhibition of specific genes downstream of apoptosis, consistent with the biological processes predicted by functional enrichment analysis.

There is often a relative balance between bone formation and bone resorption in the normal human body, and an imbalance between these two aspects, such as a decrease in bone formation or an increase in bone resorption, can lead to osteoporosis [40,41]. We established an OVX mouse model to verify the protective effect of THJGC on bone loss in vivo.The results showed that THJGC could against bone loss induced by OVX in mice indeed. Consistently, the data from micro-CT analysis demonstrated that OVX resulted in a reduction in BV/TV, Tb.Thand Tb.N, as well as an increase in Tb.Sp, whereas THJGC partially reversed these changes.In particular, we found that THJGC significantly improved the BMD of OVX mice, which is a significant predictor to assess osteoporosis.In view of the results of our bioinformatics analysis, molecular docking and experiments above, we reasonably infer that the potential signal pathway network regulated by THJGC. Western blotting results showed that THJGC affected several important osteogenic and osteoclastic markers such as Runx2, NFATc1, RANKL. As we all know, in osteoporosis, they have been reported to be closely related to osteogenesis and osteoclastic differentiation. This suggests that THJGC can treat osteoporosis by promoting bone formation and attenuating unbalanced bone resorption, thereby improving bone mineral density and biomechanical properties and reducing bone microstructural degradation. However, a deeper validation requires a large number of experiments to verify, such as osteoblast and osteoclast induced differentiation experiments. This in turn can be further investigated as a separate point.

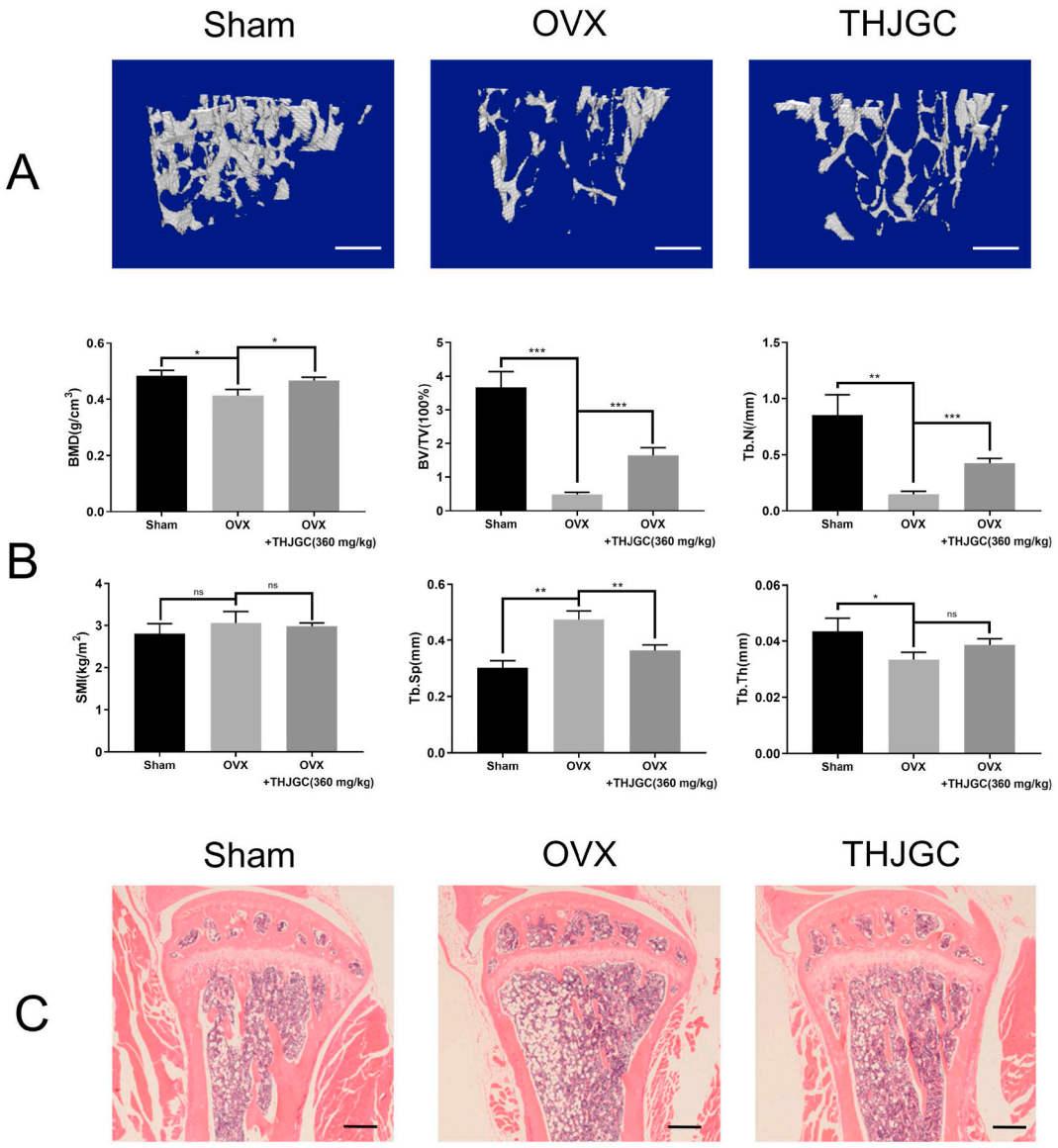

Fig. 10. THJGC protects against OVX-induced bone loss in vivo. (A)Representative three-dimensional micro-CT images of the upper end of ipsilateral tibia from sham (n = 6), OVX (n = 6), and THJGC (n = 6) groups. Scale bar = 200 μm. (B) Related important parameters such as BV/TV, Tb.N, Tb.Sp, Tb.Th, BMD, and SMI. (C) Decalcification and paraffin embedding of scanned tibial tissue and HE staining of excised thin layers (n = 6). Scale bar = 200 μm. All data was demonstrated as mean ± SD, *P < 0.05, **P < 0.01, ***P < 0.001, ****P < 0.0001vs. OVX groups.

Unfortunately, our study reveals Akt1, ERK1/2 and JNK1 signaling pathways, but it does not go far enough. In our network analysis, we showed that THJGC has not only anti-apoptotic and antioxidant effects, but also positive aspects in anti-inflammatory and angiogenic aspects in osteoporosis, however, our study focused on the former, which will be a motivation to continue our research. Overall, our study suggests that THJGC can resist bone loss by a pathway mechanism involving at least the Akt1, JNK1 and ERK1/2 signaling pathways.

5. Conclusions

Our data demonstrate for the first time that THJGC can treat osteoporosis after ovariectomy in mice.THJGC also attenuates H_2O_2-induced MC3T3-E1 oxidative damage and apoptosis by inhibiting ROS production. These may be accomplished by regulating the Akt1, ERK1/2 and JNK1 pathways(Fig. 11). Our findings provide a new perspective for exploring the potential approach of THJGC in the treatment of osteoporosis or even other bone metabolic diseases.

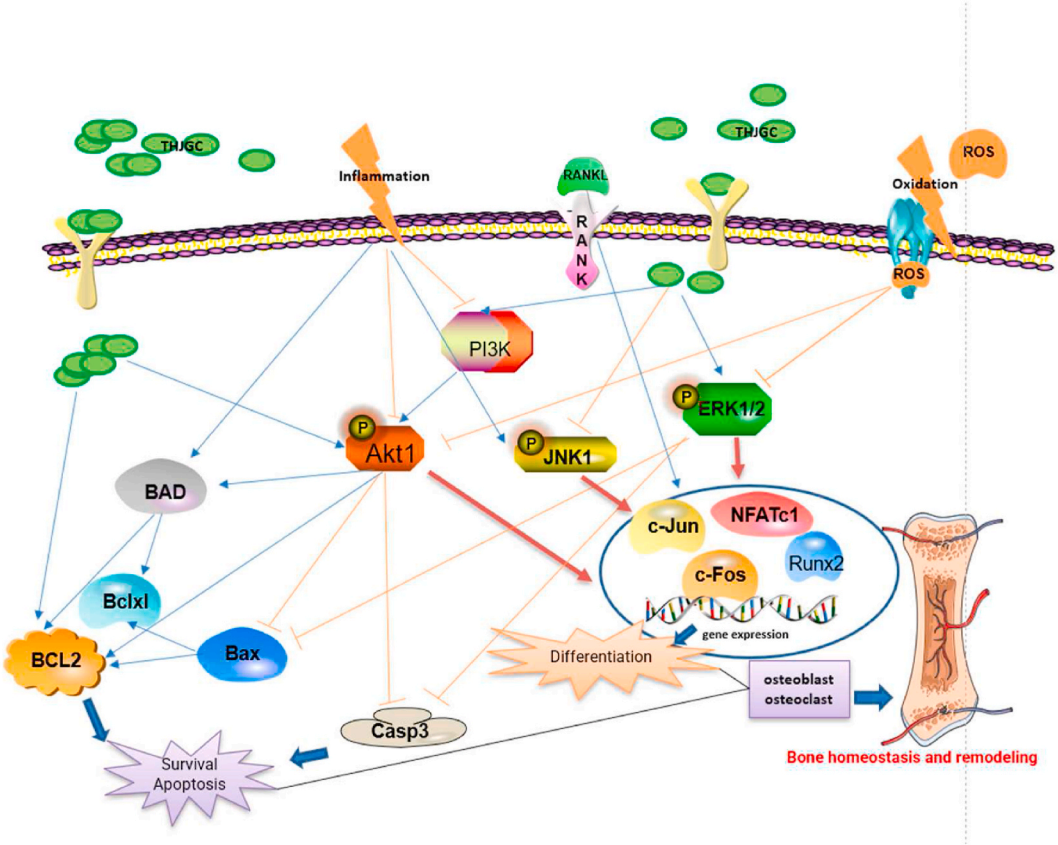

Fig. 11. The main possible mechanisms of THJGC against osteoporosis. Key ingredients including quercetin, luteolin, and kaempferol were identified.

Ethics statement

All animal experiments were handled and used according to the acceptance standards of the Ethics Committee of Guangzhou University of Chinese Medicine (approval number: 20,220,426,002).

Funding

This study was supported by the National Natural Science Foundation of China (No: 82074462, 82004395); Shenzhen Futian District Health and Public Welfare Scientific Research Project (FTWS2020058); Henan Scientific and Technological Research Project (No: 222102310124); the Joint Construction Project of Henan Provincial Health Committee and Ministry of Health (No: LHGJ20210035).

Author contribution statement

Miao Li; Hongyu Tang; Meng Zhang: Conceived and designed the experiments; Wrote the paper.
Yuanhao Hu; Songtao Li; Pan Kang; Baihao Chen; Shaocong Li: Performed the experiments; Analyzed and interpreted the data.
Haibin Wang; Shaochuan Huo: Conceived and designed the experiments; Contributed reagents, materials, analysis tools or data.

Data availability statement

Data will be made available on request.

Declaration of competing interest

The authors declare that they have no known competing financial interests or personal relationships that could have appeared to influence the work reported in this paper.

Appendix A. Supplementary data

Supplementary data to this article can be found online at https://doi.org/10.1016/j.heliyon.2023.e19812.

References

[1] J.A. Kanis, et al., European guidance for the diagnosis and management of osteoporosis in postmenopausal women, Osteoporos. Int. 24 (1) (2013) 23–57.
[2] P.N. Kannegaard, et al., Excess mortality in men compared with women following a hip fracture. National analysis of comedications, comorbidity and survival, Age Ageing 39 (2) (2010) 203–209.
[3] T. Sözen, L. Özışık, N. Başaran, An overview and management of osteoporosis, Eur J Rheumatol 4 (1) (2017) 46–56.
[4] M.R. McClung, et al., Odanacatib for the treatment of postmenopausal osteoporosis: results of the LOFT multicentre, randomised, double-blind, placebo-controlled trial and LOFT Extension study, Lancet Diabetes Endocrinol. 7 (12) (2019) 899–911.
[5] S.W. Wang, et al., Steroidogenic effect of Erxian decoction for relieving menopause via the p-Akt/PKB pathway in vitro and in vivo, J. Ethnopharmacol. 195 (2017) 188–195.
[6] F. Gu, et al., An experimental research into the potential therapeutic effects of Anti-Osteoporosis Decoction and Yougui Pill on ovariectomy-induced osteoporosis, Am J Transl Res 11 (9) (2019) 6032–6039.
[7] L.P. Zhou, et al., Bone protective effects of danggui buxue Tang alone and in combination with tamoxifen or raloxifene in vivo and in vitro, Front. Pharmacol. 9 (2018) 779.
[8] F.X. Bing, et al., Clinical Study on Tenghuang Jiangu Capsules Combined with Zoledronic Acid in Treatment of Senile Primary Osteoporosis, Drugs & Clinic, 2018.
[9] Z. Shuyun, M.A. Suying, Clinical Study of Tenghuangjiangu Capsule Combined with Warm Acupuncture in Treatment of Primary Osteoporosis, Chinese Journal of Traditional Medical Traumatology & Orthopedics, 2018.
[10] I.R. Indran, et al., Preclinical studies and clinical evaluation of compounds from the genus Epimedium for osteoporosis and bone health, Pharmacol. Ther. 162 (2016) 188–205.
[11] S.N. Kang, et al., In vitro anti-osteoporosis properties of diverse Korean Drynariae rhizoma phenolic extracts, Nutrients 6 (4) (2014) 1737–1751.
[12] H.D. Liang, et al., Cistanches Herba aqueous extract affecting serum BGP and TRAP and bone marrow Smad1 mRNA, Smad5 mRNA, TGF-β1 mRNA and TIEG1 mRNA expression levels in osteoporosis disease, Mol. Biol. Rep. 40 (2) (2013) 757–763.
[13] C. Liu, et al., Rehmanniae Radix in osteoporosis: a review of traditional Chinese medicinal uses, phytochemistry, pharmacokinetics and pharmacology, J. Ethnopharmacol. 198 (2017) 351–362.
[14] T.H. Kim, et al., The effects of luteolin on osteoclast differentiation, function in vitro and ovariectomy-induced bone loss, J. Nutr. Biochem. 22 (1) (2011) 8–15.
[15] S.K. Wong, K.Y. Chin, S. Ima-Nirwana, The osteoprotective effects of kaempferol: the evidence from in vivo and in vitro studies, Drug Des Devel Ther 13 (2019) 3497–3514.
[16] Y. Xu, et al., Icariin promotes osteogenic differentiation by suppressing Notch signaling, Eur. J. Pharmacol. 865 (2019), 172794.
[17] J. Ru, et al., TCMSP: a database of systems pharmacology for drug discovery from herbal medicines, J Cheminform 6 (2014) 13.
[18] J.S. Amberger, A. Hamosh, Searching online mendelian inheritance in man (OMIM): a knowledgebase of human genes and genetic phenotypes, Curr Protoc Bioinformatics 58 (2017), 1.2.1-1.2.12.
[19] G. Stelzer, et al., The GeneCards suite: from gene data mining to disease genome sequence analyses, Curr Protoc Bioinformatics 54 (2016), 1.30.1-1.30.33.
[20] D. Szklarczyk, et al., The STRING database in 2021: customizable protein-protein networks, and functional characterization of user-uploaded gene/measurement sets, Nucleic Acids Res. 49 (D1) (2021) D605–d612.
[21] P. Shannon, et al., Cytoscape: a software environment for integrated models of biomolecular interaction networks, Genome Res. 13 (11) (2003) 2498–2504.
[22] S.M. Rizvi, S. Shakil, M. Haneef, A simple click by click protocol to perform docking: AutoDock 4.2 made easy for non-bioinformaticians, Excli j 12 (2013) 831–857.
[23] A.B. Chokshi, M.T. Chhabria, P.R. Desai, Rational discovery of novel squalene synthase inhibitors through pharmacophore modelling, Curr. Comput. Aided Drug Des. 14 (3) (2018) 221–233.
[24] S. Reagan-Shaw, M. Nihal, N. Ahmad, Dose translation from animal to human studies revisited, Faseb j 22 (3) (2008) 659–661.
[25] D. Chen, et al., 12-Deoxyphorbol 13-acetate inhibits RANKL-induced osteoclastogenesis via the attenuation of MAPK signaling and NFATc1 activation, Int Immunopharmacol 101 (Pt A) (2021), 108177.
[26] J.A. Kanis, et al., The effect on subsequent fracture risk of age, sex, and prior fracture site by recency of prior fracture, Osteoporos. Int. 32 (8) (2021) 1547–1555.
[27] J. Sun, et al., Quercetin attenuates osteoporosis in orchiectomy mice by regulating glucose and lipid metabolism via the GPRC6A/AMPK/mTOR signaling pathway, Front. Endocrinol. 13 (2022), 849544.
[28] S.K. Wong, K.Y. Chin, S. Ima-Nirwana, Quercetin as an agent for protecting the bone: a review of the current evidence, Int. J. Mol. Sci. 21 (17) (2020).
[29] Z. Jing, et al., Luteolin attenuates glucocorticoid-induced osteoporosis by regulating ERK/Lrp-5/GSK-3β signaling pathway in vivo and in vitro, J. Cell. Physiol. 234 (4) (2019) 4472–4490.
[30] W.S. Lee, et al., Kaempferol inhibits IL-1β-stimulated, RANKL-mediated osteoclastogenesis via downregulation of MAPKs, c-Fos, and NFATc1, Inflammation 37 (4) (2014) 1221–1230.
[31] A.R. Sharma, J.S. Nam, Kaempferol stimulates WNT/β-catenin signaling pathway to induce differentiation of osteoblasts, J. Nutr. Biochem. 74 (2019), 108228.
[32] E.K. Kim, E.J. Choi, Pathological roles of MAPK signaling pathways in human diseases, Biochim. Biophys. Acta 1802 (4) (2010) 396–405.
[33] A. Mukherjee, P. Rotwein, Selective signaling by Akt1 controls osteoblast differentiation and osteoblast-mediated osteoclast development, Mol. Cell Biol. 32 (2) (2012) 490–500.
[34] J. He, et al., Therapeutic anabolic and anticatabolic benefits of natural Chinese medicines for the treatment of osteoporosis, Front. Pharmacol. 10 (2019) 1344.
[35] V. Domazetovic, et al., Oxidative stress in bone remodeling: role of antioxidants, Clin Cases Miner Bone Metab 14 (2) (2017) 209–216.
[36] X. Gan, et al., Blockade of Drp1 rescues oxidative stress-induced osteoblast dysfunction, Biochem. Biophys. Res. Commun. 468 (4) (2015) 719–725.
[37] K. Schröder, NADPH oxidases in bone homeostasis and osteoporosis, Free Radic. Biol. Med. 132 (2019) 67–72.
[38] M.M. Juntilla, et al., AKT1 and AKT2 maintain hematopoietic stem cell function by regulating reactive oxygen species, Blood 115 (20) (2010) 4030–4038.
[39] S.E. Oh, M.M. Mouradian, Cytoprotective mechanisms of DJ-1 against oxidative stress through modulating ERK1/2 and ASK1 signal transduction, Redox Biol. 14 (2018) 211–217.
[40] J.B. He, M.H. Chen, D.K. Lin, New insights into the tonifying kidney-yin herbs and formulas for the treatment of osteoporosis, Arch Osteoporos 12 (1) (2017) 14.
[41] T. Wang, et al., Therapeutic potential and outlook of alternative medicine for osteoporosis, Curr. Drug Targets 18 (9) (2017) 1051–1068.